

Vision Reimagined: AI-Powered Breakthroughs in WiFi Indoor Imaging

Jiayang Shi^{1,4}, Bowen Zhang², Amartansh Dubey³, Ross Murch³ *Fellow, IEEE*
and Liwen Jing^{1,3}

¹Faculty of Information and Intelligence, Shenzhen X-Institute, Shenzhen, China

²College of Big Data and Internet, Shenzhen Technology University, Shenzhen, China

³Department of Electronic and Computer Engineering, the Hong Kong University of Science and Technology, Hong Kong, China

⁴School of Computer Science and Technology, Harbin Institute of Technology (Shenzhen)

Indoor imaging is a critical task for robotics and internet-of-things. WiFi as an omnipresent signal is a promising candidate for carrying out passive imaging and synchronizing the up-to-date information to all connected devices. This is the first research work to consider WiFi indoor imaging as a multi-modal image generation task that converts the measured WiFi power into a high-resolution indoor image. Our proposed WiFi-GEN network achieves a shape reconstruction accuracy that is 275% of that achieved by physical model-based inversion methods. Additionally, the Fréchet Inception Distance score has been significantly reduced by 82%. To examine the effectiveness of models for this task, the first large-scale dataset is released containing 80,000 pairs of WiFi signal and imaging target. Our model absorbs challenges for the model-based methods including the non-linearity, ill-posedness and non-certainty into massive parameters of our generative AI network. The network is also designed to best fit measured WiFi signals and the desired imaging output. For reproducibility, we will release the data and code upon acceptance.

Index Terms—WiFi imaging, Generative AI, Inverse Scattering Problem

I. INTRODUCTION

THE perception of indoor environment for robots, intelligent devices and systems is becoming increasingly important for every household, office building, industrial plant and other indoor facilities nowadays. Such information is crucial in the following ways: (1) facilitating the navigation and coordination of different types of robots and smart devices, (2) benefiting household care for elderly, children and even pets with real-time monitoring, (3) improving security by accurate invasion detection and anomaly alerts, (4) improving the service performance of indoor intelligent systems and etc. Utilizing the omnipresent WiFi signal for indoor imaging and localization is attracting wide attention because it is cost-effective, privacy-friendly and device-free for the target[1][2][3][4]. Comparing with image sensor based methods, WiFi signal can only detect limited information of the target, e.g. location, shape, material, movement and etc[5][6]. Consequently, users' personal information is protected by default without the need of privacy-preserving computation. WiFi sensing is also a passive sensing method, which means no extra device is required for target objects. At the same time, phaseless WiFi imaging only require very simple modification of WiFi access points, so that this approach requires minimum resources for deployment comparing with other techniques like LiDAR, RADAR, camera, 5G, ultra wide band (UWB) signals and etc [7][8]. Beyond the aforementioned advantages, WiFi is also the most commonly used method of network connection, so that information acquired through WiFi signals can spread and share among all connected devices easily.

This work has been submitted for potential publication. Copyright may be transferred without notice. Jiayang Shi and Bowen Zhang contributed equally to this work. (Corresponding author: Liwen Jing, email: ljing@connect.ust.hk)

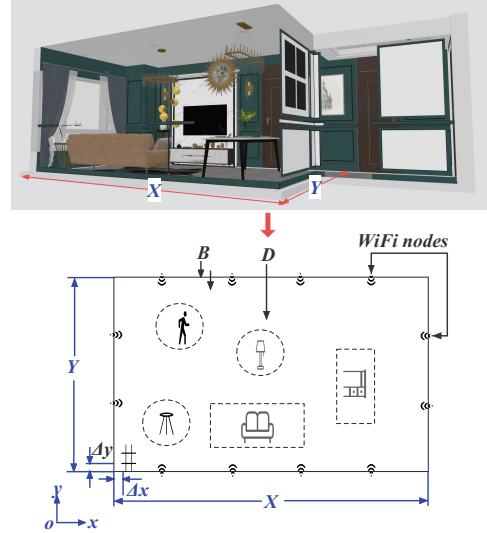


Fig. 1. DoI with wireless transceiver nodes at its boundary B and dimensions $X \times Y$ at cross-sectional height h . The transmitters and receivers are located at the boundary B . The whole area D is discretized into pixels by Δx and Δy .

The nature of indoor imaging with WiFi power measurements involves converting the measured power matrix into an image. Existing research explored full-wave (i.e. measure both WiFi phase and power) and phaseless measurements for solving indoor imaging. However, phase measurement for full-wave method is very tricky and expensive at high frequency, which makes it impractical to deploy in practice. Recent research proved the feasibility of indoor imaging by

solving phaseless inverse scattering problems using only the power measurements of WiFi signals[9][10]. Recent publications have advanced model-based methods by addressing the physical equations governing wave propagation [11][10] and integrating deep learning models with physical principles [9][5]. These methods still show limited range of applicability because they heavily rely on wave physics and the problem formulation is non-linear and ill-posed.

In this work, we construct a novel end-to-end solution for WiFi phaseless imaging by utilizing generative AI techniques for the first time. The core challenge of this task is to generate an accurate and high-resolution image by limited measurements from WiFi nodes, which enhances the performance of all tasks including indoor imaging, localization and trace tracking. In order to select an appropriate AI framework, it is also important to analyze the features of the network input and output. For this task, the measured power matrix is the input matrix, and the matrix describing the output image pixels is the output matrix. The input matrix is denser than the output matrix in practice because any element within the input matrix contains more information because it is the summation of all direct, reflected, scattered, and diffracted waves coming from the entire environment. While the output matrix only outlines the shape of indoor objects. These features are very similar to the image generation task in Dalle, Mid-journey and etc[12][13]. Consequently, in this work, we solve WiFi indoor imaging problem under the framework of multi-modal image generation for the first time.

In this work, a novel WiFi-GEN network is proposed for indoor WiFi imaging. The main contributions include:

- (1) This is the first research work to consider WiFi indoor imaging as a multi-modal image generation task that converts the measured WiFi power into a high-resolution indoor image, which advances the research field of WiFi indoor imaging.
- (2) The first customized generative AI model called WiFi-GEN network is proposed in this work for WiFi indoor imaging tasks, which eases the challenges of non-linearity, ill-posedness and uncertainty of traditional physical solutions.
- (3) A dataset of two-dimensional object shape versus WiFi power measurements has been constructed with 80000 set of data, which provides convenience for researchers to design better algorithm for this task.
- (4) Extensive experiments have been carried out to test the proposed WiFi-GEN network. The shape reconstruction accuracy of our WiFi-GEN network reaches 275% of the level attained by traditional physical model-based inversion methods, and the Fréchet Inception Distance score is reduced by 82%. At the same time, the performance of our generated results is better in terms of higher resolution and larger imaging range with fewer number of WiFi nodes.

Related work is reviewed in section II to help readers better understand the research progress in related field. Method is introduced in section III, followed by the presentation of simulation and experimental results in section IV. Conclusion and future work are discussed in section V.

II. RELATED WORK

Using WiFi signal for indoor imaging was first introduced by [1][14] for wireless inspection through the wall. Then similar work was published using moving robots to acquire measurements [2]. Initial work proved the feasibility of using WiFi signal for indoor imaging, localization, pose recognition and etc. The imaging accuracy has been improved by solving inverse scattering problems (ISP) for electromagnetic waves[5][10][15]. Inverse scattering problems are a class of problems that involve determining the properties of an object by measuring the scattered waves it produces. There are two types of ISPs which are full-wave ISP (also called full-data ISP (FD-ISP)) and phaseless ISP (PD-ISP). FD-ISPs utilize both power and phase measurements to reconstruct the target object, while PD-ISPs only need to measure WiFi power. PD-ISP is more practical to deploy because measuring WiFi power only requires simple modifications of traditional WiFi nodes, but phase measurement needs expensive network analyzers and high accuracy synchronization process. Deep learning models have been adopted to solve ISPs, which has further pushed the performance to another level [16][17].

A. Full-data and phaseless inverse scattering problems for WiFi indoor imaging

Inverse scattering problems attract attention in both theoretical and practical research disciplines. In addition to the theoretical framework built up by mathematicians, ISP techniques have also been applied in medical imaging, geophysics, radar, sonar and non-destructive testing for decades [18][19]. Recent years have seen progress in ISPs using electromagnetic waves for indoor imaging [15][10].

One approach is to acquire very precise full-wave measurements with sensor nodes surrounding the domain of interest (DOI) and formally solve ISPs considering all wave phenomenon including reflection, scattering and diffraction. However, these approaches are impractical to measure, computationally intensive and only effective in a confined environment within a few wavelengths [19][20][16]. These drawbacks limit the commercial application of FD-ISP approach in WiFi indoor imaging.

To ease the high requirement for measurement equipment, methods based on phaseless WiFi measurements have been proposed. PD-ISPs are more ill-posed and non-linear with unknown underlying physics model. An extended Rytov phaseless imaging approach demonstrated promising results in tasks including localization, imaging and identifying object materials [10]. The performance is further improved by incorporating deep learning networks to estimate unknown physics models [5].

B. The application of deep learning models in WiFi indoor imaging

Due to challenges of ill-posedness, non-linearity, complexity and uncertainty in ISPs for WiFi imaging, researchers utilize a variety of deep learning models to either estimate physics parameters in ISPs or directly reconstruct the object within

DoI. Intensive research works have been published on incorporating deep learning models in FD-ISPs [4] [15][21][22][23] and typical networks for image applications like convolutional neural network (CNN), generative adversarial network (GAN), and etc. have all been attempted. U-net CNN was adopted in [22] for direct inversion, backpropagation, and dominant current schemes. GAN was applied in [4] for inhomogeneous background imaging. Also Switchnet has been proposed to approximate forward and inverse maps arising from the time-harmonic wave equation in [21]. Although these algorithms cannot solve the innate challenge for taking full-wave measurements, they are still inspiring to show that deep learning can assist in solving wave scattering problems.

Two research works have been published on utilizing deep learning for PD-ISP. In [9], U-net CNN was chosen and three different inputs and training schemes have been compared, including direct inversion with phaseless measurement data, retrieval dominant induced currents by the Levenberg–Marquardt method, and PD with contrast source inversion scheme. Results show that without incorporating physics equations into the model, direct conversion from measured power of 16 transmitters and 32 receivers cannot provide accurate results. In [5], deep neural networks are embedded into extended Rytov approximation, and learn physical parameters iteratively. Despite the deep learning network can be a powerful tool for model-based solutions. However, in published works, none of the physical models can reconstruct hollow objects for high permittivity, and hence a deep learning network assisted by these models cannot provide satisfactory results. Physics-assisted deep-learning networks require an input of the initial reconstruction with the physical model, which might result in loss of some non-linear features and hence it can be better to directly learn all the non-linearity through a direct inversion network. At the same time, during the process of solving the model, regularization parameter needs fine-tuning under different circumstances and if correct value of regularization parameter is not used, then deep learning network don't work. The two papers mentioned above are most related to our proposed method, and [9] is the only published work that attempts to solve PD-ISP using a deep learning-based method with only the measured power as the network input. The proposed U-net in [9] extracts and saves features in the downsampling process and concatenates the feature map to the upsampling process for restoration of the original image. However, the direct conversion method results in unsatisfactory accuracy [16][5][22][9]. One possible explanation is that the conventional U-net structure is only good at identifying the main features of the input and cannot deal with subtleties in recovering the actual picture. At the same time, traditional U-net is normally implemented for tasks with similar input and output dimensions, which leads to low-resolution results in published work [9].

Our work considers the WiFi imaging task as a cross-modal generation problem. The measured WiFi power can be represented as a small matrix input that needs to be converted into the image domain, which typically has many more pixels than the input dimension. This work attempts to tackle the PD-ISP problem by using a direct inversion approach with

a generative model, without the assistance of physics models. The reason is that deep learning networks are innately good at solving non-linear and ill-posed problems by absorbing them into massive parameters, and generative models are better suited for image generation and recovery tasks. A detailed model is explained in section III.

III. PROBLEM FORMULATION AND METHOD

A. Problem Formulation

Consider a typical indoor environment with a domain of interest $D \subset \mathbb{R}^2$ with rectangular shape of $X \times Y$ m² as shown in Fig. 1. WiFi nodes are placed at its boundary (denoted as $B \subset \mathbb{R}^2$). In order to obtain measurements for PD-ISP, each WiFi node needs to measure the signal power transmitted from all other nodes separately. Current WiFi devices can be configured to work as both transmitter and receiver, so the measurement matrix \mathbf{W} obtained from M nodes has the largest dimension of $M \times M - 1$. In practice, all M nodes take turns to act as the transmitter. While one of the nodes transmits, all other $M - 1$ nodes measure the received power coming from a constant transmitting power level. This configuration is similar to conventional works in this research field [10]. Some published works configure WiFi nodes to be only transmitter or receiver [9]. However, current WiFi devices are transceivers by default, and using all nodes for both transmitting and receiving can collect more comprehensive data with fewer nodes.

The PD-ISP aims to identify the material parameter (e.g. permittivity) in each cell of the discretized 2-D DoI of $\mathbf{I}(N_x \times N_y)$, where $N_x = X/\Delta x$ and $N_y = Y/\Delta y$. For better resolution, $N_x \times N_y$ is normally much larger than $M \times M - 1$, and the increase of N_x and N_y can provide more details in the DoI. For imaging task, detecting the shape is the priority, so in this work we only reconstruct the object shape rather than the material permittivity. Consequently, the final task is generating the $N_x \times N_y$ binary matrix \mathbf{I} from the measured input matrix $\mathbf{W}(M \times M - 1)$. We consider the PD-ISP as a new cross-modal image generation problem and design a generative model called WIFI-GEN to visualize indoor objects through WiFi signals.

B. WiFi-GEN

Inspired by cross-model image generation [24], [25], [26], a novel WiFi-GEN network is proposed for end-to-end WiFi indoor imaging. Our proposed model consists of three components: (1) a WiFi signal encoder that maps WiFi signals to latent space; (2) a hierarchical control signal network for WiFi signal feature extraction; and (3) a WiFi generator for final image generation. Specifically, the WiFi signal encoder embeds WiFi signals into a square latent space matrix through a learnable fully connected network. The control signal network extracts WiFi signal-related features from the latent space and transforms them into 512-dimensional multi-level feature vectors. The WiFi generator utilizes features extracted from various levels of the control signal network to influence the final image generation outcome. For clarity, the WIFI-GEN architecture is shown in figure 2.

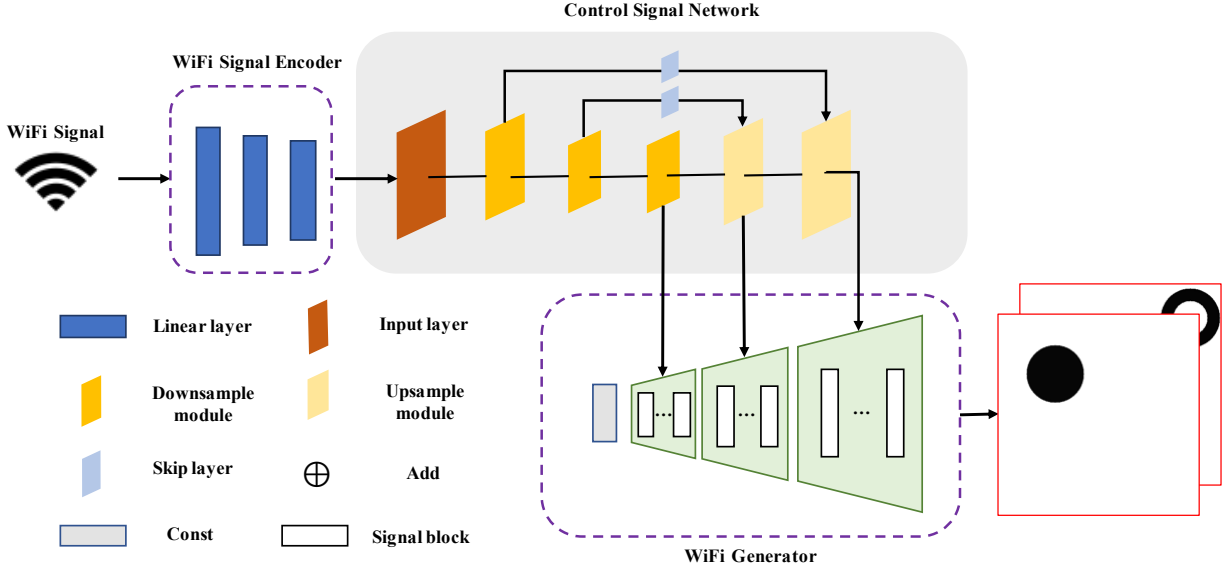


Fig. 2. Framework of our proposed WiFi-GEN, where Downsample, Upsample and Signal Block are illustrated in detail in Figure 3. Both input layer and skip layer consist of simple fully convolutional network.

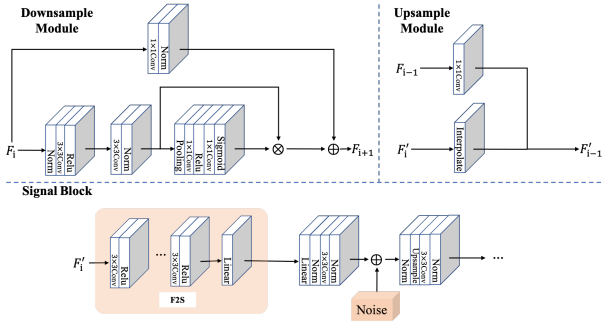


Fig. 3. Structure details of Downsample, Upsample and Signal Block in WiFi-GEN. F_i denotes the feature extracted by the i -th downsample module, F'_i denotes the feature extracted by the i -th upsample module.

WiFi Signal Encoder. The WiFi signal encoder aims to compress WiFi signals into a latent space. The information contained in WiFi power measurements is normally redundant for pure imaging task, because the power measurements include all wave phenomenon of incident, scattered and etc. Compressing the WiFi signals from the signal space to a lower dimensional latent space so as to capture the key information of the signals is necessary to achieve end-to-end accurate sensing.

The WiFi signal encoder is a three-layer fully-connected network. We flatten the 19×20 signal into a 380-dimensional vector and feed it to the encoder. Since each row of the signal matrix represents signals received by one node from others, the flattened vector preserves nodes' ordinal relations. The processed input retains information from the raw signals. The encoded signal is embedded into a 16×16 latent space for further feature extraction needed for image generation.

Control Signal Network. Control signal network extracts features of the original signal from the latent space in order to control the accuracy of final imaging. Current research

work [26], [27], [28] shows that good feature extraction can effectively improve the quality of image generation. Considering the significant differences in the shape and size of the imaging objects, we design a hierarchical feature extraction backbone with a UNet-like structure [29] using a feature pyramid [30]. This architecture can effectively extract multi-scale features from the latent space. The network architecture comprises two main components: a downsample module and an upsample module. The downsample module, located in the first half of the network, is composed of multiple residual layers designed to reduce the spatial dimensions of the feature maps. Conversely, the upsample module, situated in the second half, utilizes convolution layers and bilinear interpolation to restore the spatial resolution of the feature maps. A visual representation of the network structure can be found in Figure 3. To obtain the feature maps that govern the final image perception effect, we extract the feature maps from layers 4, 21, and 24 of the downsample module. Subsequently, these extracted feature maps are passed through the upsample layer for the WiFi generation stage.

WiFi Generator. The WiFi generator employs a method that utilizes multi-scale features extracted from the latent space to generate the ultimate image. Motivated by StyleGAN [31], [32] framework for generative adversarial networks, the WiFi generator comprises multiple signal blocks, each playing a crucial role in the generation process. Particularly, a simple yet effective feature2signal (F2S) structure is developed with multiple convolution operations to convert the input features into 512-dimensional vectors. The number of convolution layers employed for feature extraction varies depending on the depth of the features, with 6 layers used for shallow features, 5 layers for intermediate features, and 4 layers for deep features. Subsequently, these vectors are fed into the image perception module, responsible for generating the final image through a layer-by-layer process involving convolution and upsampling.

The detailed structure of the signal block in WiFi generator can be found in Figure 3. In line with established practices in generative models, we introduce noise between the different image perception modules. This deliberate introduction of noise influences the model’s ability to perceive smaller objects, as demonstrated in section IV-B.

C. Loss Function

In order to ensure the accuracy of the generated image shape, we introduce L_2 Loss to provide pixel-level generation supervision, with the specific form as follows,

$$L_2(\mathbf{W}) = \|\mathbf{I}_{gen} - \text{WiFi-GEN}(\mathbf{W})\|_2 \quad (1)$$

where \mathbf{W} represents the measurement matrix of WiFi power, and \mathbf{I}_{gen} denotes the ground truth image of the indoor environment. In order to further measure the difference between two images and maintain the quality of imaging during training, we introduce LPIPS loss, which is defined as follows,

$$L_{LPIPS}(\mathbf{W}) = \|F(\mathbf{I}_{gen}) - F(\text{WiFi-GEN}(\mathbf{W}))\|_2 \quad (2)$$

where F is a pre-trained perceptual feature extractor.

The overall objective function of WiFi-GEN is calculated as a weighted sum of the above two loss functions as follows:

$$\mathcal{L}(\mathbf{W}) = \mathcal{L}_2 + \gamma \mathcal{L}_{LPIPS} \quad (3)$$

where γ is a hyper-parameter.

IV. SIMULATION AND EXPERIMENTAL RESULTS

A. Experimental Setup and Parameter Settings

Setup: To evaluate the efficacy of our proposed method, we conducted experiments within a confined space of 3×3 m², outfitted with 20 WiFi nodes. These nodes, operating at a frequency of 2.4GHz, were positioned along the perimeter of the room, equidistant from each other. During testing, a singular node would transmit signals while the remaining 19 nodes functioned as receivers, measuring the received signal strength. Consequently, this setup generated a data matrix with dimensions of 19×20 for each measurement. The objective of our algorithm is to accurately reconstruct the room’s original environment, with the Domain of Interest (DoI) corresponding to the full area of 3×3 m². The intended outcome of this reconstruction process is a binary image with a resolution of 256×256 pixels, effectively delineating the contours of objects within the indoor space.

We used a simulation program to generate datasets for training and evaluating our generative models, creating image-WiFi measurement pairs for diverse scenario analysis. These results are in section IV-B. Additionally, real-world tests with 20 ADALM-PLUTO radios in a lab setting, akin to the study in [5] but with fewer WiFi nodes, further validated our method. Details on these physical experiments are in section IV-C.

Datasets: Addressing the substantial data requirements for training generative models, we recognized that manually collecting extensive experimental data in traditional physical environments would be prohibitively labor-intensive. To overcome this challenge, we opted for simulated data to build our

experimental dataset. Utilizing existing methods capable of translating imaging results into simulated WiFi signals, we established a novel approach for dataset construction. Our process began with the selection of four distinct object shapes: circles, squares, triangles, and rings. Each shape was assigned a random size and positioned randomly within the pixel space. This procedure yielded 20,000 unique data sets per shape. Subsequently, the simulated imaging results were converted into binary images through threshold segmentation. In these images, the areas representing objects were set to black, while the remaining space was in white. This approach not only streamlined the data generation process but also ensured a diverse and comprehensive dataset, crucial for the robust training and evaluation of our generative model. 80% of the data are used for model training, and the other 20% are used for numerical experiments.

Parameter Setting: For the training phase of our model, we utilized a 19×20 matrix representing the WiFi signal as the input. The output from the model was configured to be a 256×256 pixel image, representing the generated imaging result. The learning rate is set to 0.0001. The batch size is 8 and the hyper-parameter γ is set to 0.8. All models underwent training on a high-performance NVIDIA RTX A6000 GPU, equipped with 48 GB of memory. The model takes 7 days to complete training over 50 epochs.

Evaluation Metrics: Two parameters are selected to evaluate the performance including Fréchet inception distance (FID) and the Intersection over Union (IoU). FID is the widely used metric in image generation to measure the model performance [33]. IoU is used to evaluate the accuracy of the generated image shape and position. The calculation formula for IoU is as follows,

$$IoU = \frac{\mathbf{I}_{gen} \cap \mathbf{I}}{\mathbf{I}_{gen} \cup \mathbf{I}} \quad (4)$$

Here, the intersection area is the overlapping area between the generated object boundary and the true object boundary, while the union area is the total area of the two boundaries.

Model	IoU \uparrow	FID \downarrow
Physical	-	436.752
Physical-60	0.289	-
Physical-256	0.305	270.486
Ours	0.795	79.675

TABLE I

IOU AND FID RESULTS OF OUR PROPOSED MODEL IN COMPARISON WITH PHYSICAL MODEL-BASED METHODS.

B. Comparison to Traditional Methods

In order to evaluate the performance of WiFi-GEN in the WiFi indoor imaging task, we conduct a comprehensive comparison with the state-of-the-art physical model-based methods. Results comparison of selected cases with different object shapes are shown Figure 4. Quantitative results are given in Table I and Table II, where 20% of the WiFi power and image pairs are used for experiments including 16000 set of data in all four shapes. Our methods outperforms traditional physical model-based method in three ways: (1) overall, our

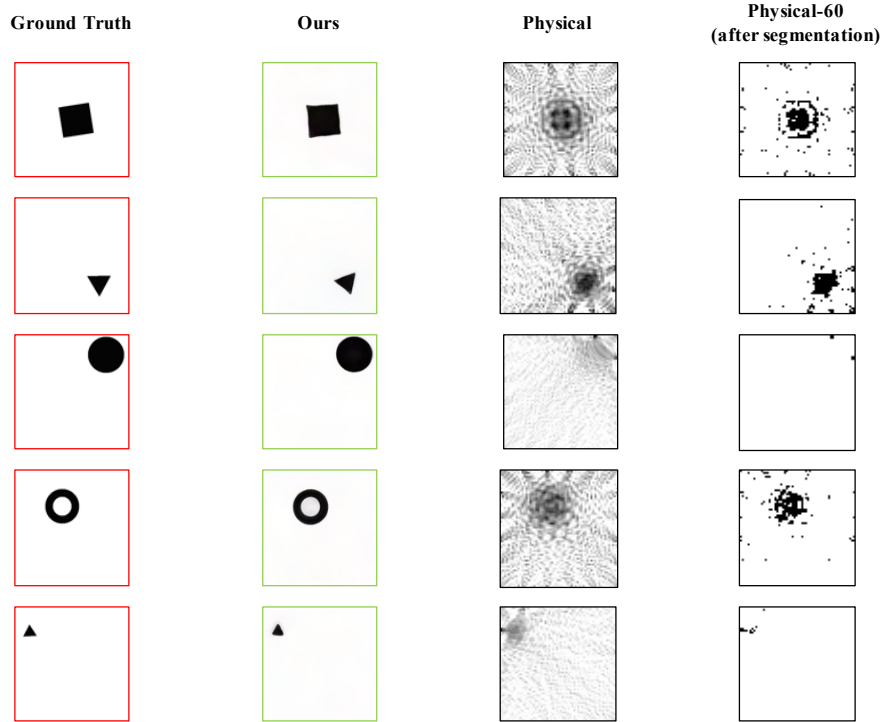


Fig. 4. Performance of selected cases of our model in comparison with physical model-based methods. Our model demonstrates substantial improvement in shape reconstruction accuracy.

Model	circle	rectangle	triangle	ring
Physical-60	0.287(\times 1.0)	0.392(\times 1.0)	0.278(\times 1.0)	0.201(\times 1.0)
Physical-256	0.3(\times 1.05)	0.416(\times 1.06)	0.296(\times 1.06)	0.21(\times 1.04)
Ours	0.841(\times 2.93)	0.836(\times 2.13)	0.777(\times 2.79)	0.728(\times 3.62)

TABLE II

IOU SCORES FOR FOUR DISTINCT SHAPES. OUR PROPOSED APPROACH DEMONSTRATES A SUBSTANTIAL ENHANCEMENT IN PERFORMANCE ACROSS ALL CATEGORIES, RANGING FROM TWO TO THREE TIMES. NOTABLY, THE RING, WHICH IS THE MOST CHALLENGING SHAPE TO PERCEIVE, EXHIBITED A REMARKABLE 3.62-FOLD ACCURACY COMPARING WITH PHYSICAL METHODS.

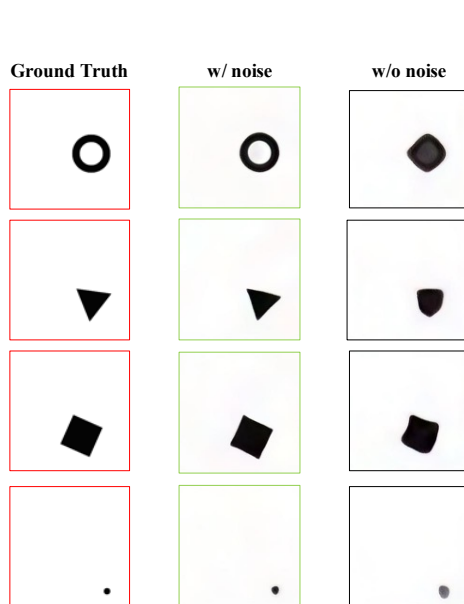


Fig. 5. Image generation capability with different noise condition in model training, where w/ refers to with, w/o refers to without

	IoU \uparrow	FID \downarrow
w/o noise	0.743	129.91
w/ noise	0.795	79.675

TABLE III

QUANTITATIVE RESULTS OF IMAGE GENERATION CAPABILITY UNDER DIFFERENT NOISE CONDITION IN MODEL TRAINING.

proposed method achieves a 275% accuracy in shape reconstruction (reflected by IoU) compared with traditional physics-based methods, and significantly lowers the FID score by 82%. At the same time, our proposed method avoided the noise problem in the final image generation. (2) Our model perform well for the most challenging non-convex shapes, and 3.62-fold accuracy is achieved in ring shapes comparing with physical methods. (3) Our method perform effectively for cases near the boundary. These cases are challenging for physical models because physical model normally assume to solve wave equation in the far-field so that it exhibits limited accuracy in regions within one wavelength to the WiFi nodes.

Post processing for model-based method: We observed that the outcomes from physical model-based methods suffer

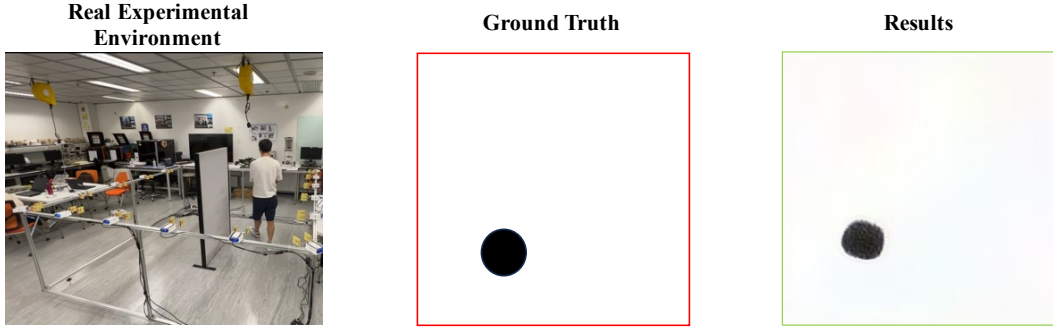


Fig. 6. Results of our method on human perception in real environments.

	Signal Frequency (GHz)	DoI Size	Relative Permittivity ϵ_r	Number of WiFi Nodes	Resolution of Recovered Image
Xu et al. [9]	0.4	$2.67\lambda \times 2.67\lambda$	1.1-1.8	16 Transmitters and 32 Receivers	32×32
Dubey et al. [11]	2.4	$12.5\lambda \times 12.5\lambda$	$1.1+0.1i$ to $77 + 7i$	40 Transceivers	60×60
WiFi-GEN	2.4	$25\lambda \times 25\lambda$	$4+0.4i$ and $77+7i$	20 Transceivers	256×256

TABLE IV
PERFORMANCE COMPARISON WITH PUBLISHED WORK.

from significant noise. To address this, we employed threshold segmentation to extract the most salient regions detected by these methods. In the results, Physical refers to the original results from physical model-based method, Physical-60 refers to physical results of 60×60 pixels after segmentation, and Physical-256 refers to the results re-sampled to 256×256 pixels after segmentation.

Shape reconstruction accuracy: It is important to highlight that our proposed method exhibits a superior imaging capability compared to model-based methods. While traditional methods only support 60×60 resolution results, our method effortlessly generates perceptual images at a resolution of 256×256 . A more detailed comparison of specific method characteristics as presented in Table IV. The visual inspection clearly demonstrates the remarkable accuracy of our method in imaging, with the ability to accurately depict four distinct object shapes as shown in Figure 4. The quantitative results obtained from the comparison experiments are summarized in Table I. These experimental findings clearly demonstrate the exceptional performance of WiFiGEN, surpassing the state-of-the-art in terms of FID and IoU, which means more accurate shape reconstruction and better image generation.

Performance of challenging cases: Notably, our model exhibits strong performance in capturing objects situated at the edges of the scene. Even small triangles positioned at the periphery are accurately perceived as shown in Figure 4. The analysis of the quantitative results presented in Table II reveals a notable enhancement in our method, particularly concerning the perception of challenging ring-shaped objects, compared to the traditional approach. This demonstrated that our proposed approach solves the challenge of imaging for non-convex shapes.

Noise Reduction: A noteworthy advantage of our model is its ability to mitigate the noise generated in non-object areas during perception, which is a challenge often encountered by traditional physical methods. These noise artifacts

are notoriously difficult to effectively remove, even through segmentation. In summary, WiFi-GEN demonstrates a highly significant performance improvement compared to traditional physical methods.

Performance improvement by introducing noise in model training: To further assess the effectiveness of incorporating noise during the model training process, we conducted a set of experiments comparison. The results presented in Figure 5 and Table III demonstrate that the inclusion of noise in model training significantly improves the ability of the model for handling small and non-convex objects.

Comparison with Published Work: Results are also compared with related work in terms of operating frequency, DoI size, object material permittivity, number of WiFi nodes and final image resolution, as shown in Table IV.

C. Physical Experiment

To assess the robustness of our model, we build an experimental setup in the laboratory that closely resemble the simulated scenario. The experimental setup is deployed with a DoI of $3 \times 3 m^2$ with 20 ADALM-PLUTO software-defined radio devices mounted on a racket at the boundary with even space, which is similar to the conventional experiments in [5] with less WiFi nodes. As illustrated in Figure 6, our model exhibits a remarkable capability to effectively comprehend the data obtained from the real scene measurement. Despite variations in the distribution of Wi-Fi signals emitted by the devices in the real environment, which differs from our simulated dataset, our model accurately captures the shape and spatial location of the devices present in the scenes, particularly exemplified by its accurate depiction of the shape and placement of the human body.

V. CONCLUSIONS AND FUTURE WORK

This work proves the feasibility and opens up great possibilities of using generative AI methods for enhancing WiFi

indoor imaging. This is a research area traditionally dominant by physicists solving wave equations. The introduction of generative AI into this research area solves the long existing challenges of ill-posedness, non-linearity and non-certainty in such problems. The proposed WiFi-GEN network outperforms the traditional physical method by roughly 3 times in terms of shape reconstruction accuracy, and also provides higher resolution and larger imaging DOI. Real-life experiments in a laboratory prove that a pre-trained model can adept to practical environments with slightly different pre-assumptions.

Future research could extend to multi-object imaging, real-time indoor systems, reducing WiFi node requirements, material detection and developing 3D imaging models.

REFERENCES

- [1] F. Adib and D. Katabi, "See through walls with wifi!" in *Proceedings of the ACM SIGCOMM 2013 conference on SIGCOMM*, 2013, pp. 75–86.
- [2] S. Depatla, L. Buckland, and Y. Mostofi, "X-ray vision with only wifi power measurements using rytov wave models," *IEEE Transactions on Vehicular Technology*, vol. 64, no. 4, pp. 1376–1387, 2015.
- [3] L. Zhao, H. Huang, W. Wang, and Z. Zheng, "An accurate approach of device-free localization with attention empowered residual network," *Applied Soft Computing*, vol. 137, p. 110164, 2023.
- [4] X. Ye, Y. Bai, R. Song, K. Xu, and J. An, "An inhomogeneous background imaging method based on generative adversarial network," *IEEE Transactions on Microwave Theory and Techniques*, vol. 68, no. 11, pp. 4684–4693, 2020.
- [5] S. Deshmukh, A. Dubey, D. Ma, Q. Chen, and R. Murch, "Physics assisted deep learning for indoor imaging using phaseless wi-fi measurements," *IEEE Transactions on Antennas and Propagation*, vol. 70, no. 10, pp. 9716–9731, 2022.
- [6] A. Dubey and R. Murch, "Distorted wave extended phaseless rytov iterative method for inverse scattering problems," *IEEE Transactions on Geoscience and Remote Sensing*, 2023.
- [7] Q. Niu, M. Li, S. He, C. Gao, S.-H. Gary Chan, and X. Luo, "Resource-efficient and automated image-based indoor localization," *ACM Transactions on Sensor Networks (TOSN)*, vol. 15, no. 2, pp. 1–31, 2019.
- [8] N. El-Sheimy and Y. Li, "Indoor navigation: State of the art and future trends," *Satellite Navigation*, vol. 2, no. 1, pp. 1–23, 2021.
- [9] K. Xu, L. Wu, X. Ye, and X. Chen, "Deep learning-based inversion methods for solving inverse scattering problems with phaseless data," *IEEE Transactions on Antennas and Propagation*, vol. 68, no. 11, pp. 7457–7470, 2020.
- [10] A. Dubey, P. Sood, J. Santos, D. Ma, C.-Y. Chiu, and R. Murch, "An enhanced approach to imaging the indoor environment using wifi rssi measurements," *IEEE Transactions on Vehicular Technology*, vol. 70, no. 9, pp. 8415–8430, 2021.
- [11] A. Dubey, S. Deshmukh, L. Pan, X. Chen, and R. Murch, "A phaseless extended rytov approximation for strongly scattering low-loss media and its application to indoor imaging," *IEEE Transactions on Geoscience and Remote Sensing*, vol. 60, pp. 1–17, 2022.
- [12] Z. Shi, X. Zhou, X. Qiu, and X. Zhu, "Improving image captioning with better use of captions," *arXiv preprint arXiv:2006.11807*, 2020.
- [13] R. Rombach, A. Blattmann, D. Lorenz, P. Esser, and B. Ommer, "High-resolution image synthesis with latent diffusion models," in *Proceedings of the IEEE/CVF conference on computer vision and pattern recognition*, 2022, pp. 10 684–10 695.
- [14] M. Zhao, T. Li, M. Abu Alsheikh, Y. Tian, H. Zhao, A. Torralba, and D. Katabi, "Through-wall human pose estimation using radio signals," in *Proceedings of the IEEE conference on computer vision and pattern recognition*, 2018, pp. 7356–7365.
- [15] Y. Wang, Z. Zong, S. He, R. Song, and Z. Wei, "Push the generalization limitation of learning approaches by multi-domain weight-sharing for full-wave inverse scattering," *IEEE Transactions on Geoscience and Remote Sensing*, 2023.
- [16] X. Chen, Z. Wei, L. Maokun, P. Rocca *et al.*, "A review of deep learning approaches for inverse scattering problems (invited review)," *ELECTROMAGNETIC WAVES*, vol. 167, pp. 67–81, 2020.
- [17] S. Kamyab, Z. Azimifar, R. Sabzi, and P. Fieguth, "Survey of deep learning methods for inverse problems," *arXiv preprint arXiv:2111.04731*, 2021.
- [18] R. D. Murch, "Inverse scattering and shape reconstruction." 1990.
- [19] X. Chen, *Computational methods for electromagnetic inverse scattering*. Wiley Online Library, 2018, vol. 244.
- [20] R. Bates, V. Smith, and R. D. Murch, "Manageable multidimensional inverse scattering theory," *Physics Reports*, vol. 201, no. 4, pp. 185–277, 1991.
- [21] Y. Khoo and L. Ying, "Switchnet: a neural network model for forward and inverse scattering problems," *SIAM Journal on Scientific Computing*, vol. 41, no. 5, pp. A3182–A3201, 2019.
- [22] Z. Wei and X. Chen, "Deep-learning schemes for full-wave nonlinear inverse scattering problems," *IEEE Transactions on Geoscience and Remote Sensing*, vol. 57, no. 4, pp. 1849–1860, 2018.
- [23] Y. Sanghvi, Y. Kalepu, and U. K. Khankhoje, "Embedding deep learning in inverse scattering problems," *IEEE Transactions on Computational Imaging*, vol. 6, pp. 46–56, 2019.
- [24] X. Huang, M.-Y. Liu, S. Belongie, and J. Kautz, "Multimodal unsupervised image-to-image translation," in *Proceedings of the European conference on computer vision (ECCV)*, 2018, pp. 172–189.
- [25] J.-Y. Zhu, R. Zhang, D. Pathak, T. Darrell, A. A. Efros, O. Wang, and E. Shechtman, "Toward multimodal image-to-image translation," *Advances in neural information processing systems*, vol. 30, 2017.
- [26] J. Shi, H. Zhang, D. Zhou, and Z. Zhang, "Toward intelligent interactive design: A generation framework based on cross-domain fashion elements," in *Proceedings of the 31st ACM International Conference on Multimedia*, ser. MM '23. New York, NY, USA: Association for Computing Machinery, 2023, p. 7152–7163. [Online]. Available: <https://doi.org/10.1145/3581783.3612376>
- [27] E. Richardson, Y. Alaluf, O. Patashnik, Y. Nitzan, Y. Azar, S. Shapiro, and D. Cohen-Or, "Encoding in style: a stylegan encoder for image-to-image translation," in *Proceedings of the IEEE/CVF conference on computer vision and pattern recognition*, 2021, pp. 2287–2296.
- [28] O. Tov, Y. Alaluf, Y. Nitzan, O. Patashnik, and D. Cohen-Or, "Designing an encoder for stylegan image manipulation," *ACM Transactions on Graphics (TOG)*, vol. 40, no. 4, pp. 1–14, 2021.
- [29] O. Ronneberger, P. Fischer, and T. Brox, "U-net: Convolutional networks for biomedical image segmentation," in *Medical Image Computing and Computer-Assisted Intervention—MICCAI 2015: 18th International Conference, Munich, Germany, October 5-9, 2015, Proceedings, Part III 18*. Springer, 2015, pp. 234–241.
- [30] T.-Y. Lin, P. Dollár, R. Girshick, K. He, B. Hariharan, and S. Belongie, "Feature pyramid networks for object detection," in *Proceedings of the IEEE conference on computer vision and pattern recognition*, 2017, pp. 2117–2125.
- [31] T. Karras, S. Laine, M. Aittala, J. Hellsten, J. Lehtinen, and T. Aila, "Analyzing and improving the image quality of stylegan," in *Proceedings of the IEEE/CVF conference on computer vision and pattern recognition*, 2020, pp. 8110–8119.
- [32] T. Karras, S. Laine, and T. Aila, "A Style-Based Generator Architecture for Generative Adversarial Networks," *arXiv:1812.04948 [cs, stat]*, Mar. 2019.
- [33] M. Heusel, H. Ramsauer, T. Unterthiner, B. Nessler, and S. Hochreiter, "Gans trained by a two time-scale update rule converge to a local nash equilibrium," *Advances in neural information processing systems*, vol. 30, 2017.